JOURNAL OF PROPULSION AND POWER
Vol. 22, No. 6, November–December 2006

Low Vulnerable Sheet Explosive Based on 3-Nitro-1,2,4-triazol-5-one

T. Mukundan,* J. K. Nair,† G. N. Purandare,‡ M. B. Talawar,§
T. Nath,§ and S. N. Asthana‖
High Energy Materials Research Laboratory, Sutarwadi, Pune 411 021, India

DOI: 10.2514/1.12697

Nitrotriazolone incorporated sheet explosives were prepared and evaluated with respect to their explosive characteristics as well as mechanical and thermal behavior. 1,3,5-Trinitro-1,3,5-triaza-cyclohexane (RDX)/Estane (85:15) composition (density, 1.23 g/cm^3 and tensile strength, 0.5 MPa) was taken as reference and the effect of replacement of RDX by nitrotriazolone to the extent of 5–25% was studied. Inclusion of nitrotriazolone led to a remarkable increase in density (1.23 → 1.41 g/cm^3) and mechanical properties (tensile strength: 0.46 → 1.08 MPa). The major finding was increase in velocity of detonation by about an average 700 m/s over the reference composition. Velocity of detonation realized ranged from 6800 to 6900 m/s for RDX/nitrotriazolone/Estane compositions. As regards sensitivity, nitrotriazolone-based compositions were relatively less vulnerable to impact and friction stimuli. Shock sensitivity of RDX/nitrotriazolone/Estane composition was also found to be of the order of 98–110 kbar as against 77 kbar for reference. The armor protection capability of nitrotriazolone-based composition against shaped charge was found to be at par with the corresponding RDX-based sheet explosive. Thermal studies revealed that nitrotriazolone and RDX incorporated sheet explosives with Estane binder decomposed as a unified composite, despite their widely differing decomposition/ignition temperatures.

Introduction

PLASTIC bonded explosives (PBX) in the form of flexible sheet explosive find wide applications in the field of welding, cladding, and demolition [1]. The concept of explosive reactive armor (ERA), consisting of a sandwiched sheet explosive, is also gaining importance in recent times [2] for the protection of armored vehicles like tanks. Israel has developed plastic bonded sheet explosives based reactive armor BLAZER [2]. Modern Russian tanks are also reported to use sheet explosives for ERA [3]. This has provided impetus to research in the field of sheet explosives. A major requirement of a sheet explosive for ERA application is that it should be initiated by a warhead jet whereas it should be immune to small caliber stimuli which the tank hull can withstand anyway. In this context, 3-nitro-1,2,4-triazol-5–1 (NTO) is a highly potential insensitive high-performance explosive. It is perhaps, the most widely evaluated explosive of this class in the recent past. It has been well studied in many pressed and cast low vulnerable explosives (LOVEX) compositions [4]. Due its explosive performance [velocity of detonation (VOD), 8500 m/s] harboring 1,3,5-Trinitro-1,3,5-triaza-cyclohexane (RDX) (VOD, 8700 m/s), and much less sensitivity, it is being projected to replace RDX fully or partly in insensitive munitions (IM).

Currently, crepe rubber is widely used as binder in sheet explosives. Rubber bonded sheet explosives have limited life due to deterioration of rubber during storage resulting in loss of flexibility and structural integrity, which is detrimental to its practical applicability. Thermoplastic elastomers (TPEs) are emerging as potential alternatives. In the present work, a TPE binder, Estane [5], has been selected as binder in view of its superior mechanical properties imparted by the suitably placed hard and soft segments in its structure. The effect of replacement of RDX by NTO on the thermophysical and sensitivity characteristics of the sheet explosive compositions was determined. The performance evaluation of the sheets developed was also undertaken during this work.

Received 12 February 2005; revision received 19 December 2005; accepted for publication 17 January 2006.

*Deputy Director and Corresponding Author; t_mukun@yahoo.com
†Scientist "C."
‡Technical Officer "B."
§Assistant Director.
‖Group Director.

Experimental

Materials

A composition containing bimodal RDX (85%; 40% of 20–30 μm and 45% of 120–212 μm) with Estane (13.5%; Number-average molecular weight (Mn): 71,809, T_g: -17°C) and dioctylphthalate (DOP, 1.5%) was taken as reference. NTO of particle size 120–212 μm was incorporated at the cost of RDX.

Method

The compositions were processed by a solvent technique [6,7]. The polymer Estane was partially gelatinized with acetone at 40–50°C with occasional stirring to get a uniform gel. The gel was transferred to a sigma blade mixer along with DOP and mixed for 10–15 min to ensure uniform distribution. Weighed quantity of RDX/NTO was added to the gel in three equal installments and mixed for 1 h at 40–50°C. During mixing, maximum of solvent evaporated leading to a dough formation. The dough was transferred to a tray and was kept for drying. After drying, it formed a cake, which was rolled at 40–50°C to get the desired thickness (5 mm) of the sheet. VOD of sheet explosives was measured by the ionization probe technique (pin oscilloscope). The impact (fall hammer-type apparatus, 2 kg weight) and friction sensitivity were determined by a Julius Peters apparatus.

Mechanical properties of these compositions in the sheet form were determined using a universal testing machine (Instron, Model 1185). A standard vacuum stability apparatus [8] was used to measure the volume of the gas generated at 100°C after 40 h from 5 g of sample. Differential scanning calorimetry (DSC) experiments were carried out on a Perkin Elmer DSC 7 instrument at a heating rate of 10°C/min in nitrogen atmosphere with a typical sample mass of 2 mg. Thermogravimetry (TG) studies were carried out on Mettler Toledo STAR instrument in nitrogen atmosphere at a heating rate of 10°C/min with a sample mass of 10 mg. Scanning electron microscope (SEM) studies were carried out on Philips SEM-EDAX instrument (model-XL 30). Theoretical prediction of VOD was

Table 1 Physico-thermal and explosive properties of RDX/NTO sheet explosives

Property	Composition			
	RDX/Estane 85:15	RDX/NTO/ Estane 80:5:15	RDX/NTO/ Estane, 70:15:15	RDX/NTO/ Estane 60:25:15
Density, g/cm^3	1.23	1.37	1.39	1.41
Theoretical VOD, m/s	6500	7100	7180	7170
Measured VOD, m/s	6150	6800	6880	6900
Impact Sensitivity $h_{50\%}$, cm	76	80	87	90
Friction sensitivity (insensitive up to, kg)	36	36	36	36
Vacuum stability (volume of gas evolved, cm^3)	0.58	0.60	0.63	0.62

performed using the BKW code [9]. Aluminium block gap test and penetration studies are given in Appendix A.

Results and Discussion

The physical, explosive, and thermal properties of the RDX/NTO sheet explosives with Estane binder in comparison with the RDX/ Estane control composition are given in Table 1. A remarkable increase in density was observed on replacement of RDX with NTO. Even 5% replacement of RDX by NTO led to an increase of 11% in density. The increase in density was about 15%, when 25% replacement was done. This is a clear indication of a better compaction of the matrix. The self-binding nature of NTO is abundantly evident in this observation. It may be attributed to the interactions between the carbonyl oxygen and azole hydrogen [10]. Hyoshi et al. [11] have established that C-O bond length of NTO in the crystal state is longer than that of an isolated molecule in the gas phase and explained it on the basis of intermolecular hydrogen bonding. The observation of peak at m/z 261 in addition to the molecular ion peak at m/z 131$(m + 1)$ in the mass spectrum is also considered an outcome of formation of a cluster ion (adduct) due to intermolecular interactions [12]. Such interactions involving azole hydrogen and $-NO_2$ groups of RDX may also be operative in the system. Role of particle size of fillers may also be significant in determining the binding nature.

Enhancement in compaction is also apparent in the SEM micrographs (Fig. 1). Figs. 1a and 1b show the surface of the control and control with 5% NTO replacement, respectively. The observed increase in density can be correlated with the difference in the close packing of the two matrices. The same surfaces at the higher magnification are shown in Figs. 1c and 1d. Fig. 1c shows tearing of the binder film resulting in a loose dispersion of solid particles of

a) SEM micrograph of control formulation, 500x

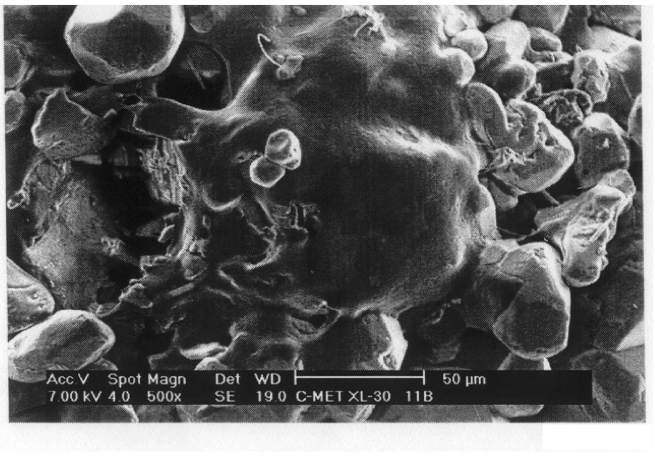

b) SEM micrograph of control composition with 5 % NTO, 500x

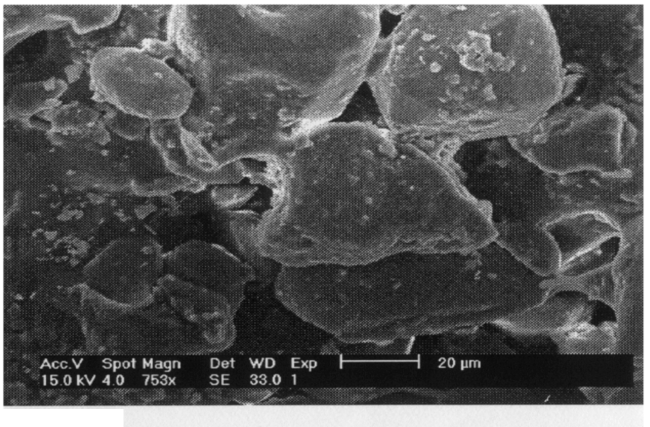

c) SEM micrograph of control composition, 750x

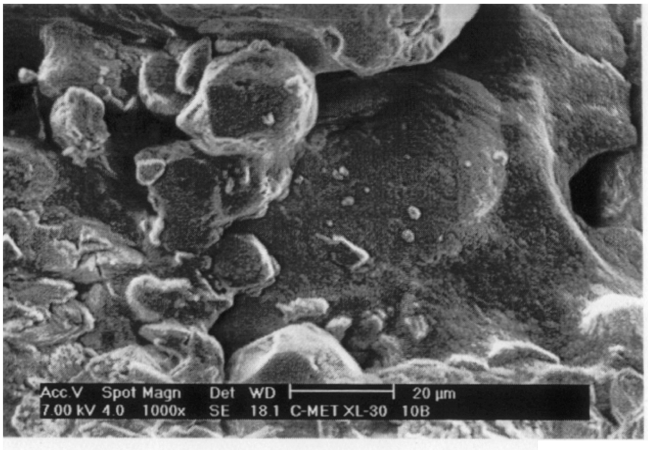

d) SEM micrograph of control with 5% NTO, 1000x

Fig. 1 SEM micrographs.

RDX leading to voids and thus low density. Such defects are not visible in Fig. 1d, wherein there is 5% NTO suggesting that the binding is definitely better.

VOD obtained for RDX/Estane (85:15) was 6150 m/s, whereas NTO/RDX/Estane compositions gave VOD ranging from 6800 to 6900 m/s. The experimentally obtained VOD of these compositions are in close agreement with the theoretically predicted values (7000–7180 m/s).

The inherent energy potential of NTO is marginally lower (ΔH_f, −117 kJ/mol and VOD, 8500 m/s) than that of RDX (ΔH_f, +71 kJ/mol and VOD, 8700 m/s). However, as mentioned, the self-binding characteristics of NTO yield composition with superior density, which may be considered a major contributing factor to higher VOD. The low sensitivity of these compositions to impact and friction stimuli was another finding of this work. In shock sensitivity tests, RDX/NTO/Estane compositions were initiated on attenuating the donor shock wave by aluminum blocks of only 25–27 mm thickness, whereas RDX/Estane composition initiated in terms of 50% probability of detonation, when attenuated by Al blocks of 31 mm thickness. These results bring out that the RDX/NTO/Estane compositions were initiated with a shock wave of 98–110 kbar, whereas the corresponding value for RDX/Estane composition was 77 kbar (Table 2). These trends may be correlated with relatively lower vulnerability of NTO to mechanical and shock stimuli.

Further, the self-binding property of NTO enables it to undergo compaction, thus absorbing shock better, leading to less sensitivity. A consolidated mass is expected to have a lower extent of microporosity, and thereby a reduction in the probability of formation of hot spots due to the adiabatic compression of entrapped air in compositions. Much higher activation energy of decomposition of NTO (300 kJ/mol) than that of RDX may also be a prominent contributing factor [12] towards lesser probability of formation and propagation of hot spots.

Table 2 Shock sensitivity (by aluminum block gap test) of sheet explosives

Composition	Height of Al block, mm	Pressure, kbar
RDX/Estane 85:15	31	77
RDX/NTO/Estane 80:5:15	27	99
RDX/NTO/Estane 70:15:15	25	110

Table 3 Mechanical properties of RDX/NTO/Estane compositions

Composition	Elongation, %	Tensile strength, MPa
RDX/Estane 85:15	65	0.46
RDX/NTO/Estane 80:5:15	38	0.71
RDX/NTO/Estane 70:15:15	28	1.03
RDX/NTO/Estane 60:25:15	21	1.08

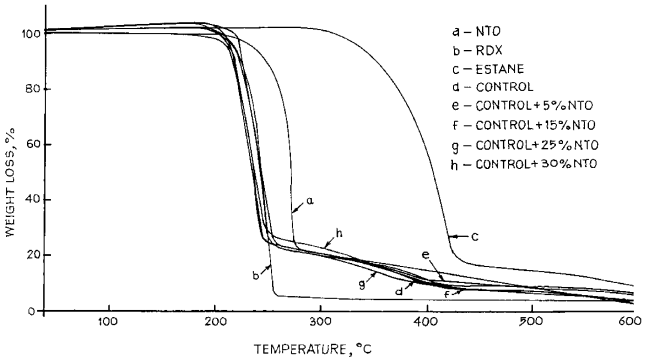

Fig. 2 TG curves of the sheet explosives and the constituents.

Superior structural integrity of the NTO-containing compositions is manifested in the mechanical properties. Thus, incorporation of 5% NTO in the composition led to a 40% increase in the tensile strength and the increase was about twofold when the NTO proportion incorporation was increased to 15–25% (Table 3).

The volume of gas evolved in vacuum stability test for RDX/NTO/Estane composition was more or less same as that of RDX/Estane composition suggesting the compatibility of NTO with RDX as well as Estane. DSC results (Table 4) suggest a concerted decomposition of RDX and NTO upon heating. All curves showed a melting peak (that of RDX) around 200–220°C, immediately followed by an exotherm with $T_{max} \approx 240$°C. On increasing the NTO content to 25–30% level, the T_{max} was marginally brought down to 236–230°C. In these cases, the Ti is also lower by 5°C. The data are thus indicative of a weak sensitization of the decomposition of the control matrix by NTO, which itself is decomposing (in the matrix) at much lower temperature than in pure form.

TG studies (Fig. 2) revealed a one-step weight loss of 80% for NTO and 95% for RDX in the temperature range 255–275°C and 205–250°C, respectively. Neat Estane binder showed a one-step weight loss of about 85% in the temperature range of 340–420°C. The control and NTO-containing compositions showed a two-step weight loss typically in the temperature ranges of 205–204°C (∼75%) and 240–400°C (∼15%). The fact that all compositions including the ones containing NTO showed a similar weight loss pattern with major decomposition starting in the region of decomposition of pure RDX (205°C) is corroborative of the observation in DSC studies. Thus, despite the different thermal stabilities of RDX and NTO in the sheet explosive, both decomposed as a unit mass.

Brill [13] has reviewed the RDX decomposition mechanism and opined that two thermally neutral pathways are operative leading to

Table 4 Thermal analysis results of the formulations

Composition	DSC		TG	
	Endotherm T_{max}, [a] °C	Exotherm T_m, °C	Temperature range, °C	Weight loss, %
RDX	205	240.5	205–250	95
NTO	——	——	255–275	78–16
RDX/Estane 85:15	203	240.5	205–204	75
			240–400	18
RDX/NTO/Estane 80:5:15	202	240.5	200–250	70
			243–400	20
RDX/NTO/Estane 70:15:15	201	239.5	200–242	72
			241–398	18
RDX/NTO/Estane 60:25:15	200	236.5	200–225	78
			240–402	17
RDX/NTO/Estane 55:30:15	200	230.0	200–250	70
			243–403	20

[a] T_{max} (peak decomposition temperature)

the formation of CH_2O and N_2O (−121 kJ/mol) and HCN and HONO (+117 kJ/mol). NTO is known to undergo thermal decomposition through C-N bond homolysis either by direct cleavage of C-NO_2 or by initial transfer of H^+ followed by C-NO_2 rupture. NO_2 free radicals generated during NTO decomposition triggers an autocatalytic process [14]. Interplay between RDX and NTO decomposition process appears responsible in triggering a concerted decomposition of the composition.

In penetration trials, the penetration observed with no ERA cartridge, was ∼350 mm. It was found that an ERA cartridge containing (5–15%) NTO and (80–70%) RDX-based sheet explosive sandwich was effective in bringing down the penetration by half. This penetration reduction level was comparable to that achieved by RDX/Estane (85/15) and RDX/HTPB (80/20) sheets. The sheet explosives containing higher percentage of NTO (20–25%) could not be initiated.

Conclusions

New sheet explosives of the type NTO/RDX/Estane have been developed. The NTO-containing sheets were found to be less sensitive to shock, impact, and friction stimuli compared with the reference RDX/Estane sheets. The NTO-containing sheets are more compact as evidenced by density and higher VOD. The mechanical properties of the new sheets are also superior to that of the reference RDX/Estane sheets. Thermal studies suggest a concerted decomposition of RDX and NTO in sheet explosive formulation. The armor protection capability of the new sheet explosive was at par with RDX-based sheet explosive. The NTO-containing sheet explosives have great potential in ERA type of applications considering the overall armor protective capability and low vulnerability as well as superior structural integrity.

Appendix: Shock Sensitivity and Penetration Studies

Aluminium Block Gap Test

Shock sensitivity was measured by the aluminum block gap test, using an in-house assembly as shown schematically in Fig. A1, by determining the minimum pressure of the shock wave that can initiate detonation in the sheet explosive (acceptor charge). A cylindrical donor charge of pressed RDX/wax (95:5) of 30-mm-diam and 100 mm length of density 1.64 g/cm^3 and VOD of 8100 m/s was used to generate the shock wave. The shock wave was allowed to pass through an aluminum block (density, 2.785 g/cm^3) of 63-mm-diam and height varying from 10 to 44 mm. The critical pressure across the aluminum block which can detonate the sheet explosive (5 mm thick) with 50% probability, has been determined using the standard equation [15], $P = 505.8e^{0.060338x}$, where P is the critical pressure in kbar and x is the thickness of the Al block in mm.

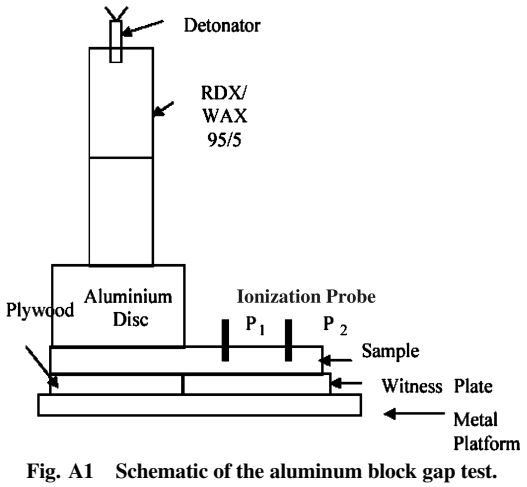

Fig. A1 Schematic of the aluminum block gap test.

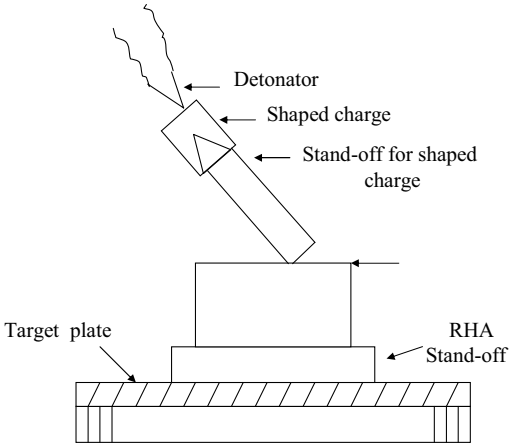

Fig. A2 Experimental setup for penetration studies.

Penetration Studies

Penetration studies were carried out using a setup shown schematically in Fig. A2. A single sheet explosive (126 × 126× 5 mm) was sandwiched between MS plates in an ERA cartridge. The cartridge was placed on a rolled homogeneous armor (RHA) target plate of 400 mm thickness. A 80 mm shaped charge was mounted at 60 deg angle. The charge was initiated by an electric (no. 33) detonator. After the trial, the target plate was cut open and the penetration was measured.

Acknowledgment

The authors thank Shri A. Subhananda Rao, Director, HEMRL for his keen interest in the work.

References

[1] Rinehart, J. S., and Pearson, J., *Explosive Working of Metals*, Pergamon, New York, 1963, pp. 149–179.
[2] Vered, G. R., "Evolution of BLAZER Reactive Armour and its Adaptation in AFVs," *Military Technology, MILTECH*, Vol. 12, No. 12, 1987, pp. 53–55.
[3] Warford, J. M., "Reactive Armour-New Life for Soviet Tanks," *Armor*, Vol. 97, No. 1, Jan.–Feb. 1988, pp. 6–22.
[4] Becuwe, A., and Delclos, A., "Low Sensitivity Explosive Compounds for Low Vulnerability Warheads," *Propellants, Explosives, Pyrotechnics*, Vol. 18, No. 1, 1993, pp. 1–10.
[5] Foltz, M. F., "Thermal Stability of ε-Hexanitrohexaazaisowurtzitane in ESTANE Formulation," *Propellants, Explosives, Pyrotechnics*, Vol. 19, No. 2, 1964, pp. 63–69.
[6] Dagley, I. J., Parkar, R. P., Montelli, L., and Louey, C. N., "Mixed High Explosives for Insensitive Booster Compositions," Materials Research Laboratory, Rept. MRL-TR-22, Victoria, Australia, 1992.
[7] Humphris, P. J., and Thompson, L. C. R., "Flexible Sheet Explosives with Low Velocities of Detonation," Australian Defence Scientific Service TM 27, Defence Standards Laboratory, Victoria, Australia, Feb. 1969
[8] Bofors, A. B., "Analytical Methods for Powders and Explosives," *Nobel Krute*, Bofors, Sweden 1960.
[9] Mader, C. L., "Fortran BKW: A Code for Computing Detonation Properties of Explosives," Los Alamos National Laboratory, Rept. LA-3704, Los Alamos, NM, 1967.
[10] Xiao, H.-M., Ju, X.-H., Xu, L.-N., and Fang, G.-Y., "A Density-Functional Theory Investigation of 3-nitro-1,2,4-triazole-5-one Dimers and Crystal," *Journal of Chemical Physics*, Vol. 121, No. 24, 2004, pp. 12523–12531.
[11] Hiyoshi, R. I., Kohno, Y., and Nakamura, J., "Vibrational Assignment of Energetic Material 5-nitro-2, 4-dihydro-1,2,4-triazole-3-one (NTO) with Labeled Isomers," *Journal of Physical Chemistry A*, Vol. 108, No. 27, 2004, pp. 5915–5920.
[12] Singh, G., and Felix, Prem. S., "Studies on Energetic Compounds Part 16. Chemistry and Decomposition Mechanism of 4-dihydro-3H-1,2,4-triazole-3-one (NTO)," *Journal of Hazardous Materials*, Vol. 81, Nos. 1–2, 2001, pp. 67–82.

[13] Brill, T. B., "Multiphase Chemistry Considerations of the Surface of Burning Nitramine Monopropellants," *Journal of Propulsion and Power*, Vol. 11, No. 4, 1995, pp. 740–751.
[14] Oxley, J. C., Smith, J. J., and Zhou, Z., "Thermal Decomposition Studies on NTO and NTO/TNT," *Journal of Physical Chemistry*, Vol. 99, No. 25, 1995, pp. 10383–10391.
[15] Yadav, H. S., Nath, T., Sundaram, S. G., Kamath, P. V., and Kulkarni, M. W., "Shock Initiation of Sheet Explosive," *Propellants, Explosives, Pyrotechnics*, Vol. 19, No. 1, 1994, pp. 26–31.

S. Son
Associate Editor